X-Ray Diffraction Study of Argon and Xenon in the Liquid State near Their Triple Points

RONALD W. HARRIS†‡ AND GLEN T. CLAYTON
Physics Department, University of Arkansas, Fayetteville, Arkansas
(Received 12 August 1966)

X-ray diffraction patterns obtained from liquid argon and liquid xenon in equilibrium with their vapors at temperatures 0.3 K° above their triple points were used to calculate the corresponding distribution functions and radial distribution functions. Isothermal compressibilities and the mean-square variations of the distance between nearest neighbors were calculated from these functions. The numbers of nearest neighbors based on ideal peak fittings were determined to be 8.52 for argon and 8.94 for xenon with peaks occurring in the undamped radial distribution functions at 3.79 and 4.38 Å, respectively. A comparison of the distribution functions for the two liquids indicates that the work is consistent. Distance ratios in the distribution functions are in good agreement with that obtained by Scott *et al.* for random-packed spheres. Intensity functions of argon were compared with the experimental work of Eisenstein and Gingrich and with the Lennard-Jones convolution-hypernetted-chain (L. J. CHNC) theoretical calculations of Khan. Similar comparisons were made for xenon with the experimental work of Campbell and Hildebrand and with the L. J. CHNC theoretical calculations of Khan and Broyles.

INTRODUCTION

THE inert elements are expected to form statistical liquids suitable for theoretical study. A summary of diffraction studies of these liquids has been given by Kruh.[1] Of these, argon is best suited for experimental investigation since it can be condensed at liquid-air temperatures and has the most favorable absorptive and scatterir g properties. Accordingly, it has received the most attention, with the work of Eisenstein and Gingrich[2] being one of the most thorough studies conducted on any liquid. Gingrich and Tompson[3] later made a study of argon in which they attempted to better determine the position of the first maximum in the radial distribution function[4] near the triple point, and they investigated the number of nearest neighbors resulting from various area-assignment techniques. Khan[5] has calculated intensity functions and distribution functions[6] from theoretical considerations and compared the results to Eisenstein and Gingrich's work.

Because of the high absorption of x rays by xenon, it remains one of the least studied of the inert element liquids. Campbell and Hildebrand[7] have presented x-ray diffraction patterns of liquid xenon at three conditions of temperature and pressure using a transmission-photographic method. Khan and Broyles[8] have calculated intensities and distribution functions from theoretical considerations and compared the results to Campbell and Hildebrand's work. The agreement between experiment and theory is poorer for xenon than that for argon, neon, or krypton, and they suggest that the experimental intensities should be remeasured.

It is the purpose of the present work to:

1. Obtain intensity patterns for liquid argon and liquid xenon near their triple points, and from them to calculate radial distribution functions (RDF) and distribution functions (DF).
2. Assign area to peaks in the RDF's on the basis of ideal peak[1,9,10] calculations.
3. Compare the DF's of argon and xenon to check the consistency of the present experimental work.
4. Compare the DF's of argon and xenon to that of random-packed spheres.[11]
5. Calculate the isothermal compressibilities from the experimental DF's of argon and xenon.
6. Calculate the mean-square variation of the distance between nearest neighbors for argon and xenon.
7. Compare the presently observed intensities and calculated DF's of argon and xenon with theoretical calculations and previous experimental work. Comparisons are made with the L. J. CHNC[12] theoretical calculations since they are available for both argon and xenon near their triple points.

EXPERIMENTAL

Diffraction patterns were obtained for $s=4\pi\lambda^{-1}\sin\theta$ $=0.3$ to 14.1 Å^{-1} by use of a theta-theta diffractometer[13] using Mo$K\alpha$ radiation. Sample conditions were main-

* This research was supported in part by funds from the National Science Foundation.
† Present address: Shell Development Company, P. O. Box 481, Houston, Texas.
‡ National Aeronautics and Space Administration Trainee.
[1] R. F. Kruh, Chem. Rev. **62**, 319 (1962).
[2] A. Eisenstein and N. S. Gingrich, Phys. Rev. **62**, 261 (1942).
[3] N. S. Gingrich and C. W. Tompson, J. Chem. Phys. **36**, 2398 (1962).
[4] Throughout this paper the term "radial distribution function" means $4\pi r^2\rho(r)$ and is designated RDF.
[5] A. A. Khan, Phys. Rev. **134**, A367 (1964).
[6] Throughout this paper the term "distribution function" means $g(r)$ and is designated DF.
[7] J. A. Campbell and J. H. Hildebrand, J. Chem. Phys. **11**, 334 (1943).
[8] A. A. Khan and A. A. Broyles, J. Chem. Phys. **43**, 43 (1965).
[9] J. Waser and V. Schomaker, Rev. Mod. Phys. **25**, 671 (1953).
[10] R. W. Harris and G. T. Clayton, J. Chem. Phys. **45**, 2681 (1966).
[11] G. D. Scott, J. D. Bernal, J. Mason, and K. R. Knight, Nature **194**, 956 (1962).
[12] Convolution-hypernetted chain equation with a Lennard-Jones interaction potential.
[13] P. C. Sharrah, J. I. Petz, and R. F. Kruh, J. Chem. Phys. **32**, 241 (1960).

tained by a system which is similar in design to that described by Petz.[14] Liquid air and liquid nitrogen were used as coolants, and a 10 W heater along with various insulating spacers placed between the sample holder and the coolant tank provided coarse temperature control. It was necessary to reduce the pressure above nitrogen-enriched liquid air in order to bring the argon sample to the triple point. Two copper-constantan thermocouples were imbedded in the sample holder; one monitored the temperature, and the other was used to provide a signal to the sensing element of an electronic control unit which maintained the temperature at the selected value to within 0.05°K. At liquid-air temperatures there was a gradient of about 0.1°K across the base of the sample holder. The curved 0.015 in. Mylar window of the sample holder did not contribute a pattern of its own since a Bragg-Brentano[15] focusing system was employed.

The triple points of argon and xenon are approximately[16,17] 84.0 and 161.2°K, respectively. Each sample was cooled slightly below its triple point temperature and allowed to begin to solidify; the solid state was detected by observation of the sharp maxima in the diffraction pattern. The sample was then slowly heated until these maxima were no longer observed. The difference between the temperature at which a combination of the solid and liquid patterns was observed and the temperature at which only a liquid pattern was observed was determined to be 0.3±0.1°K. Hence, the temperatures reported for this work are 84.3±0.1°K for argon and 161.5±0.1°K for xenon.

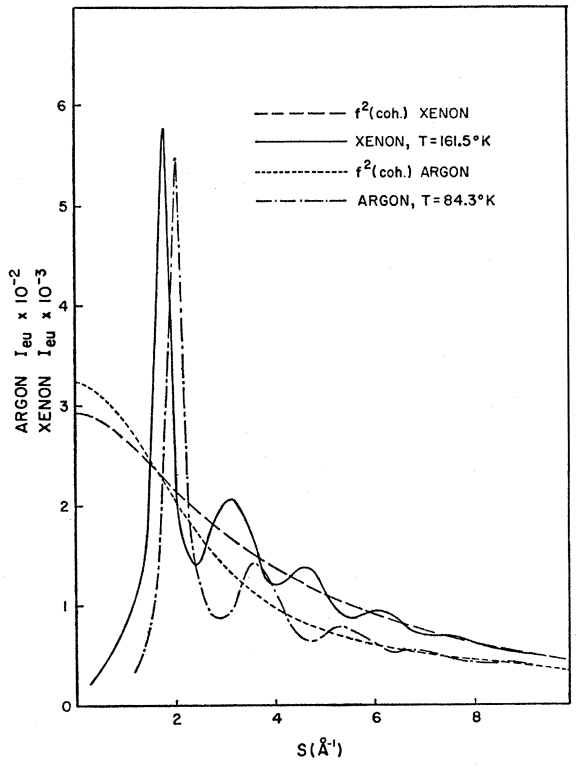

FIG. 1. Scattered intensity from argon and xenon near their triple points. The intensity functions have been corrected for polarization, absorption, incoherent scattering, and background, and have been scaled to match the coherent scattering functions at high angle.

ANALYSIS

The intensity data were corrected for polarization,[15] sample transmission,[18] incoherent scattering,[19] and background. The incoherent scattering was first corrected for recoil[20,21] and monochromator discrimination (determined experimentally). The corrected intensity was scaled to match the scattering functions[19] at high angle and are shown in Fig. 1. As a guide in scaling, the sensitive integral test[22] and Bienenstock's[23] function were used.

The RDF's were calculated from

$$4\pi r^2\rho(r)=4\pi r^2\rho_0+(2r/\pi)\times\int_0^{s_{max}} si(s)M(s)\sin(rs)ds, \quad (1)$$

where ρ_0 is the bulk atom density of the liquid, $\rho(r)$ is the atom density at a distance r from any reference atom center in the liquid, $M(s)$ is the modification function, and s_{max} was taken as 9.1 Å^{-1} for argon and 8.0 Å^{-1} for xenon. The function $si(s)$ was formed according to

$$si(s)=s(I_{eu}-f^2), \quad (2)$$

where I_{eu} is the corrected intensity in electron units, and f^2 is the atomic coherent scattering function. Since no data were taken between $s=0.0$ and $s=0.3$ Å^{-1}, $si(s)$ was extrapolated linearly to the origin beginning from the value of the function at 0.3 Å^{-1}. Following the method outlined by Kruh,[1] an $M(s)$ function was used of the form

$$M(s)=(1/f^2)e^{-bs^2}, \quad (3)$$

where b is a constant. Waser and Schomaker[9] have developed a formalism whereby the effect of intensity data modification on an interaction peak in the RDF can be determined. Such a peak can be considered to consist of a linear sum of single pair interaction peaks. These theoretical peaks are called ideal peaks and are formed

[14] J. I. Petz, J. Chem. Phys. 43, 2238 (1965).
[15] B. D. Cullity, *Elements of X-ray Diffraction* (Addison-Wesley Publishing Company, Inc., Reading, Massachusetts, 1956).
[16] Linde Rare Gases, Union Carbide Company, New York, 1953 (unpublished).
[17] *International Critical Tables* (McGraw-Hill Book Company, Inc., New York, 1926).
[18] M. E. Milberg, J. Appl. Phys. 29, 64 (1958).
[19] K. Sagel, *Tabellen zur Roentgenstrukturanalyse* (Springer-Verlag, Berlin, 1958).
[20] G. Breit, Phys. Rev. 27, 362 (1926).
[21] P. A. M. Dirac, Proc. Roy. Soc. (London) A111, 405 (1926).
[22] J. Krogh-Moe, Acta. Cryst. 9, 951 (1956).
[23] A. Bienenstock, J. Chem. Phys. 31, 570 (1959).

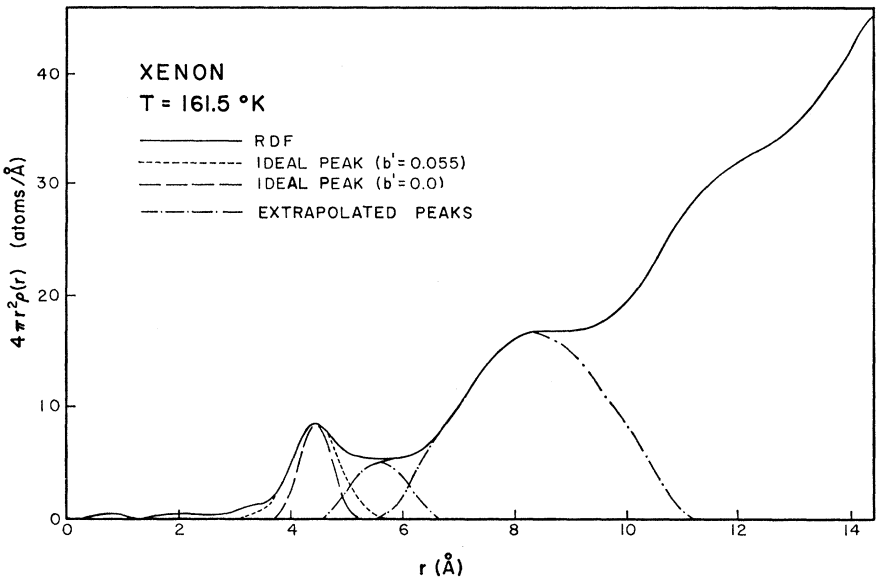

FIG. 2. The radial distribution function for xenon near its triple point. Ideal peak fittings and area assignment are shown.

according to

$$t(r)=(\pi)^{-1}\int_0^{s\max} f^2 e^{-b's^2}M(s)\cos(rs)ds, \qquad (4)$$

where b' is one half the mean-square variation of the distance between the atom pair. Calculations were made with b' equal to zero and various values of b until an ideal peak resulted which was relatively free of spurious structure. The RDF's were calculated using this value of b; the results for xenon are shown in Fig. 2. Ideal peak calculations were then made with various values of b', using the same value of b, until an ideal peak resulted which could be scaled to fit the first maximum. The area under this peak represents the number of nearest neighbors. Area was then assigned to the adjacent peaks by subtracting the ideal peak fitted at the first maximum from the RDF and extrapolating the right side of the adjacent peak to be symmetric with the left side; this process was repeated with the next adjacent peak.

The DF's were calculated according to

$$g(r)=\rho_0^{-1}\rho(r)=1+(2\pi^2\rho_0 r)^{-1}\times\int_0^{s\max} si(s)M(s)\sin(rs)ds. \qquad (5)$$

The results are shown in Fig. 3 for argon and in Fig. 4 for xenon.

As a check on the consistency of the work, DF's were plotted versus r^*, where r^* is the ratio of r to the value of r at the first maximum in $g(r)$. The results are shown in Fig. 5.

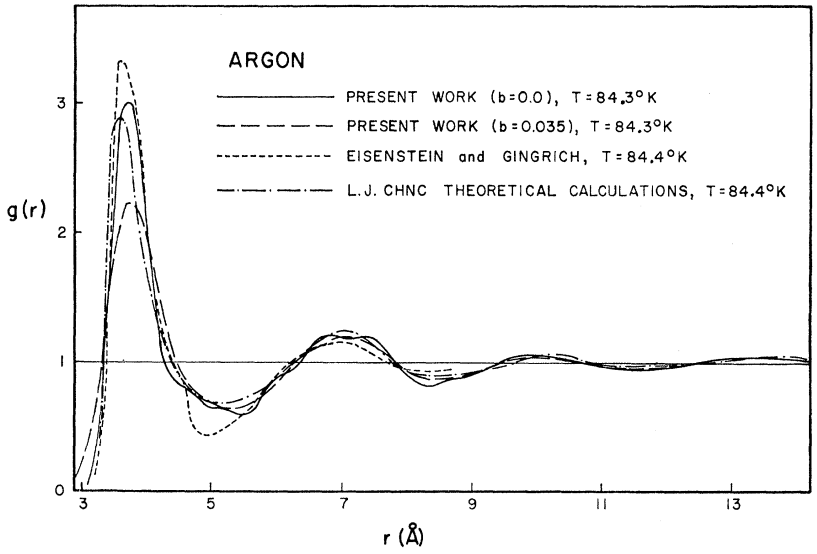

FIG. 3. The experimental distribution for argon is graphically superimposed on Khan's Fig. 6 for qualitative comparison with his L. J. CHNC theoretical calculation and with Eisenstein and Gingrich's experimental results.

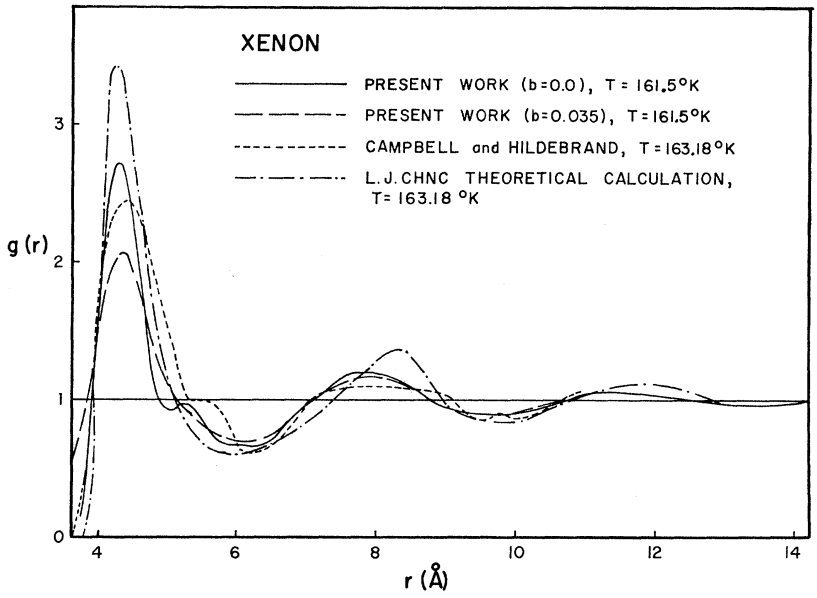

FIG. 4. The experimental distribution function for xenon is graphically superimposed on Khan and Broyles's Fig. 3 for qualitative comparison with their L. J. CHNC theoretical calculation and with Campbell and Hildebrand's experimental results.

The isothermal compressibilities were calculated from the equation[24]

$$K=(kT)^{-1}\left[(\rho_0)^{-1}+4\pi\int_0^{\infty} r^2[g(r)-1]dr\right], \quad (6)$$

where k is Boltzmann's constant and T is the absolute temperature. Since $[g(r)-1]$ converges to zero rather rapidly, the integration was carried out to an upper limit of r equal to 20.0 Å.

All calculations were made on the IBM 7040 computer at the University of Arkansas. The integrals were evaluated by means of the trapezoidal rule, applying Filon's[25] correction function where applicable.

RESULTS AND CONCLUSIONS

In accordance with the objectives set forth in the Introduction, the following results and conclusions are presented.

1. Diffraction patterns were obtained from liquid argon at 84.3±0.1°K and from liquid xenon at 161.5 ±0.1°K, each in equilibrium with its vapor, and were analyzed. The corrected intensities are shown in Fig. 1 and peak positions are given in Table I.

It was found that a damping factor with b equal to 0.035 and b' equal to zero produced an ideal peak relatively free of spurious structure and with the area to be properly associated with a single pair interaction. Therefore the RDF's were calculated using the intensity functions and scattering functions shown in Fig. 1 with this value of b. Since there were only small statistical fluctuations beyond $s=9.1$ for argon and beyond $s=8.0$ for xenon, these values were used for s_{max} in Eq. (1). The resulting RDF and ideal peak, scaled to the height of the first maximum, are shown in Fig. 2. The RDF for argon is not shown since it is similar in form to that of xenon.

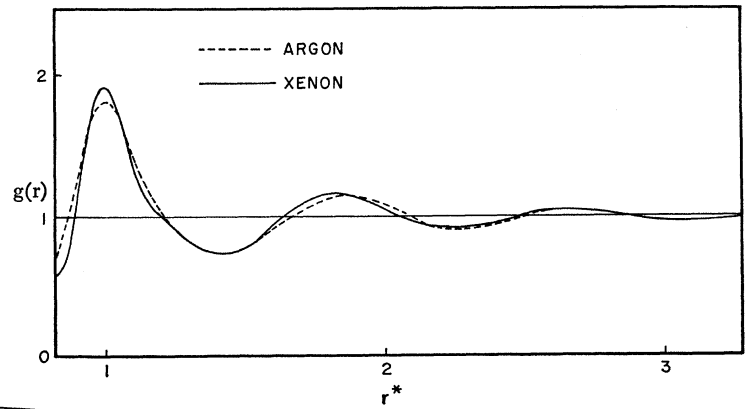

FIG. 5. As a check on the consistency of the present work, unsharpened and undamped distribution functions for argon and xenon are shown plotted versus r^*, where r^* is the ratio of r to the value of r at the first maximum in $g(r)$.

[24] A. Guinier, *X-Ray Diffraction in Crystals, Imperfect Crystals, and Amorphous Bodies* (Freeman and Company, San Francisco, 1963).
[25] L. N. Filon, Proc. Roy. Soc. (Edinburgh) 49, 38 (1928).

Using the same values for s_{max}, the DF's were calculated from Eq. (5), and the results are shown in Fig. 3 for argon and in Fig. 4 for xenon. The positions of peaks in the DF's are tabulated in Table II.

2. Area was assigned to peaks in the RDF's as outlined in the analysis section. An attempt to fit the stationary ideal peak for xenon to the first maximum in the RDF is shown in Fig. 2. The broader peak in the RDF indicates vibration. By using a value of b' equal to 0.055 and using the same value of b as used in the calculation of the RDF, an ideal peak resulted which could be scaled to fit the first maximum as shown. The area under this peak gives the number of nearest neighbors. Peak positions in the RDF and corresponding areas are given in Table III for argon and xenon. The interpretation is that peak I represents first nearest neighbors, peak III represents second nearest neighbors, and that peak II represents the probability of atoms existing between these two groups.

3. From the good agreement of the DF's for argon and xenon compared in Fig. 5, it is concluded that the experimental technique and analysis in this work yields essentially consistent results for these two elements in the liquid state.

4. The ratios of peak positions in the DF's to the position of the first peak have been tabulated and compared to those calculated by Scott[11] *et al.*, for random-packed spheres in Table IV. The very good agreement between these ratios is indicative that argon and xenon in the liquid state near the triple point pack similarly to random-packed spheres.

5. From Eq. (6) and the DF's shown in Fig. 3 and Fig. 4 (present experimental curves only), the isothermal compressibilities of argon at 84.3°K and of xenon at 161.5°K were calculated to be 133.24×10^{-11} and 79.14×10^{-11} cm²/dyne, respectively. The value of the isothermal compressibility of argon as calculated by Khan from the Lennard-Jones convolution-hypernetted-chain (L. J. CHNC) distribution function is 78.3×10^{-11} cm²/dyne.

6. From the values of b' given in Table III, the mean-square variation of the distances between nearest neighbors for argon at 84.3°K and for xenon at 161.5°K were calculated to be 0.080 Å² and 0.110 Å², respectively.

7. The intensity function for argon at 84.3°K is compared[26] in Fig. 6 with Khan's L. J. CHNC theoretical calculation and with the experimental measurements of Eisenstein and Gingrich, both curves being for 84.4°K. The height of the first peak is greater than either of the other two, although there is good agreement of position. Successive peaks are shifted to slightly smaller values of s. The present experimental intensity yields improved agreement in the shown magnitude of the maxima and minima, for peaks other than the first, with the theoretical curve.

The intensity function for xenon at 161.5°K is compared[26] in Fig. 7 to Campbell and Hildebrand's intensity measurements at 163.18°K and to the L. J. CHNC calculation of Khan and Broyles for the same temperature. The present first peak is much narrower than that of Campbell and Hildebrand, about the same width as the theoretical peak, but of lesser magnitude than either of the other two. The first minimum and second maximum are in better agreement with that of Campbell and Hildebrand in regard to position; they are of greater magnitude than Campbell and Hildebrand's peaks and of lesser magnitude than the theoretical peaks. Much better agreement with the theoretical curve occurs for successive peaks than with the intensity measurements by Campbell and Hildebrand.

DF's calculated for argon at 84.3°K with b equal to 0.035 are compared[26] in Fig. 3 to Eisenstein and Gingrich's experimental results for 84.4°K and the L. J. CHNC calculation by Khan for the same temperature. The calculation with b equal to zero was made to

TABLE I. Intensity function peak positions (Å⁻¹).

Liquid	Temp. (°K)	First	Second	Third	Fourth	Fifth
Argon	84.3	2.00	3.56	5.29	6.74	8.65
Xenon	161.5	1.73	3.12	4.58	6.04	7.50

TABLE II. Peak positions (Å) in the distribution functions ($b=0.035$).

Liquid	Temp. (°K)	First	Second	Third	Fourth	Fifth	Sixth
Argon	84.3	3.76	7.00	10.00	13.20	16.40	19.60
Xenon	161.5	4.34	7.92	11.55	14.80	18.90	···

TABLE III. Peak positions (Å) and areas (atoms) in the radial distribution functions ($b=0.035$).

		Peak I			Peak II		Peak III	
Liquid	Temp. (°K)	Position[a]	b	Area	Position	Area	Position	Area
Argon	84.3	3.87	0.040	8.52	4.94	4.46	7.50	48.86
Xenon	161.5	4.44	0.055	8.94	5.58	5.52	8.40	37.56

[a] In the undamped distributions the position of the first maximum is 3.79 Å for argon and 4.38 Å for xenon.

TABLE IV. Ratio of peak positions in the distribution functions.

Distribution	Temp. (°K)	2/1	3/1	4/1	5/1	6/1
Argon	84.3	1.86	2.66	3.51	4.46	5.22
Xenon	161.5	1.80	2.63	3.36	4.30	···
Random-packed spheres	···	1.83	2.64	3.45	···	···

[26] The figures shown for comparison were made graphically using the present results, journal figures, and enlarged figures along with tabulated data furnished by A. A. Khan and A. A. Broyles.

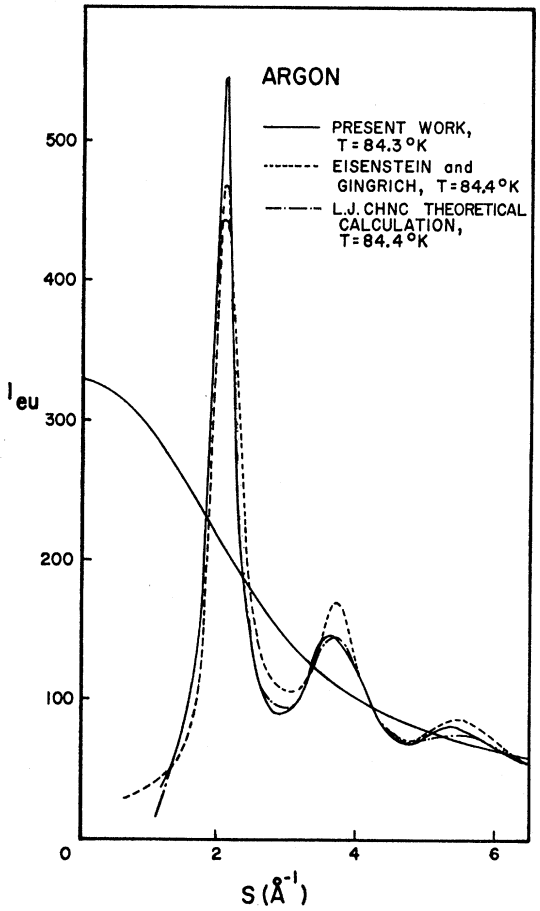

FIG. 6. In order to qualitatively compare the present work with the L. J. CHNC calculation by Khan and with Eisenstein and Gingrich's experimental measurements, the scattering function and scattered intensity for argon shown in Fig. 1 have been graphically superimposed on Khan's Fig. 19 so as to give best agreement between the scattering function shown in Fig. 1 and the one shown in Eisenstein and Gingrich's Fig. 3 from which Khan's Fig. 19 was derived.

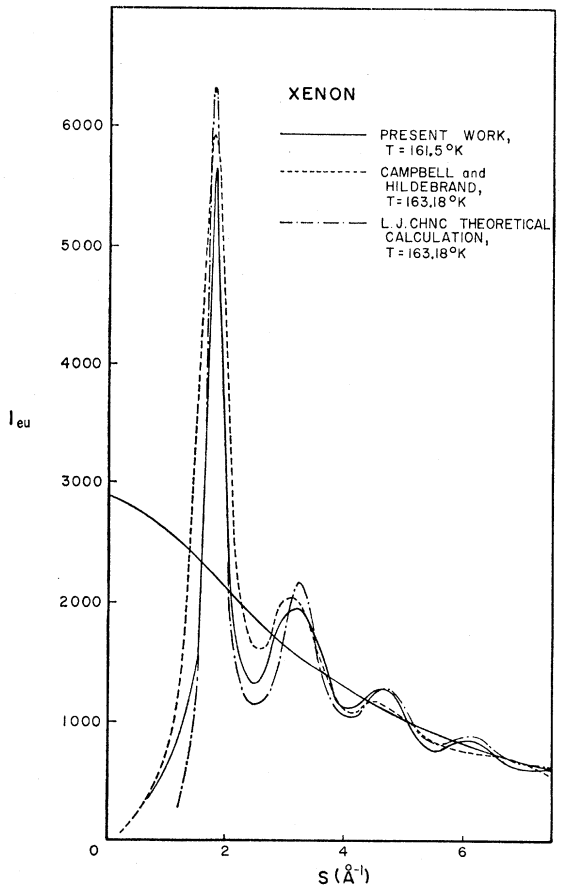

FIG. 7. In order to qualitatively compare the present work with the L. J. CHNC theoretical calculation by Khan and Broyles and with Campbell and Hildebrand's experimental measurements, the scattered intensity for xenon shown in Fig. 1 has been graphically superimposed on Khan and Broyles's Fig. 6 so as to give best agreement between the scattering function for xenon shown in Fig. 1 and the one in Khan and Broyles's Fig. 6.

fully sharpen the peaks in the DF. The undamped DF is in better agreement with the theoretical curve than with the experimental curve of Eisenstein and Gingrich. The damped DF is relatively free of spurious structure, but has a broader and lower first maximum than the undamped one.

DF's calculated for xenon at 161.5°K with b equal to 0.035 are compared[26] to Campbell and Hildebrand's experimental curves at 163.18°K and to the L. J. CHNC theoretical calculation for the same temperature by Khan and Broyles as shown in Fig. 4. The present work is in better agreement with Campbell and Hildebrand's curves in regard to position; however, the latter are broader and smaller. The theoretical peaks are considerably sharper than those calculated from experimental data and do not agree in the position of the second and third maxima.

From these comparisons it is concluded that the present work is in better agreement with the L. J. CHNC theoretical calculations than is previous experimental work. However, there is still a greater disparity between experiment and theory for xenon than for argon.

ACKNOWLEDGMENTS

Appreciation is expressed to A. A. Khan and A. A. Broyles for supplying their L. J. CHNC calculations in tabulated form.